Remote Sensing of Environment 232 (2019) 111297

Contents lists available at ScienceDirect

Remote Sensing of Environment

journal homepage: www.elsevier.com/locate/rse

A raster version of the Circumpolar Arctic Vegetation Map (CAVM)

Martha K. Raynolds[a,*], Donald A. Walker[a], Andrew Balser[b], Christian Bay[c], Mitch Campbell[d], Mikhail M. Cherosov[e], Fred J.A. Daniëls[f], Pernille Bronken Eidesen[g], Ksenia A. Ermokhina[h], Gerald V. Frost[i], Birgit Jedrzejek[j], M. Torre Jorgenson[k], Blair E. Kennedy[l], Sergei S. Kholod[m], Igor A. Lavrinenko[m], Olga V. Lavrinenko[m], Borgþór Magnússon[n], Nadezhda V. Matveyeva[m], Sigmar Metúsalemsson[n], Lennart Nilsen[o], Ian Olthof[p], Igor N. Pospelov[h], Elena B. Pospelova[h], Darren Pouliot[p], Vladimir Razzhivin[m], Gabriela Schaepman-Strub[q], Jozef Šibík[r], Mikhail Yu. Telyatnikov[s], Elena Troeva[e]

[a] Institute of Arctic Biology, University of Alaska Fairbanks, AK 99775, USA
[b] AECOM Environment, Fairbanks, AK 99701, USA
[c] Institute for Bioscience, Aarhus University, Roskilde, Denmark
[d] Nunavut Department of Environment, Arviat, Nunavut, Canada
[e] Institute of Biological Problems of the Cryolithozone, Siberian Branch of the Russian Academy of Sciences, Yakutsk, Russia
[f] Institute of Biology and Biotechnology of Plants, University of Münster, Schlossplatz 8, 48143 Münster, Germany
[g] The University Centre in Svalbard, PB 156, 9171 Longyearbyen, Norway
[h] A.N. Severtsov Institute of Ecology and Evolution, Russian Academy of Sciences, 33 Leninskiy ave., Moscow 119071, Russia
[i] ABR, Inc. —Environmental Research & Services, PO Box 80410, Fairbanks, AK 99708, USA
[j] Institute of Landscape Ecology, University of Münster, Heisenbergstraße 2, 48149 Münster, Germany
[k] Alaska Ecoscience, Fairbanks, AK 99709, USA
[l] Landscape Science and Technology, Environment and Climate Change Canada, 1125 Colonel By Drive, Ottawa, Ontario K1A 0H3, Canada
[m] Komarov Botanical Institute, Russian Academy of Sciences, Professor Popov, 2, Saint Petersburg 197376, Russia
[n] Icelandic Institute of Natural History, Urridaholtsstraeti 6-8, 212 Garðabær, Iceland
[o] University of Tromsø, Hansine Hansens veg 18, 9019 Tromsø, Norway
[p] Natural Resources Canada, 560 Rochester St., Ottawa, Ontario K1S 5K2, Canada
[q] Department of Evolutionary Biology and Environmental Studies, University of Zurich, Winterthurerstrasse 190, CH-8057 Zurich, Switzerland
[r] Plant Science and Biodiversity Center, Slovak Academy of Sciences, Institute of Botany, Bratislava, Slovak Republic
[s] Russian Academy of Science, Central Siberian Botanical Garden, Siberian Branch of the RF Academy of Science, Zolotodolinskaya str., 101, Novosibirsk 630090, Russia

ARTICLE INFO

Edited by Emilio Chuvieco

Keywords:
AVHRR
MODIS
CAVM
Land cover classification
Arctic
Arctic vegetation
Treeline

ABSTRACT

Land cover maps are the basic data layer required for understanding and modeling ecological patterns and processes. The Circumpolar Arctic Vegetation Map (CAVM), produced in 2003, has been widely used as a base map for studies in the arctic tundra biome. However, the relatively coarse resolution and vector format of the map were not compatible with many other data sets. We present a new version of the CAVM, building on the strengths of the original map, while providing a finer spatial resolution, raster format, and improved mapping. The Raster CAVM uses the legend, extent and projection of the original CAVM. The legend has 16 vegetation types, glacier, saline water, freshwater, and non-arctic land. The Raster CAVM divides the original rock-water-vegetation complex map unit that mapped the Canadian Shield into two map units, distinguishing between areas with lichen- and shrub-dominated vegetation. In contrast to the original hand-drawn CAVM, the new map is based on unsupervised classifications of seventeen geographic/floristic sub-sections of the Arctic, using AVHRR and MODIS data (reflectance and NDVI) and elevation data. The units resulting from the classification were modeled to the CAVM types using a wide variety of ancillary data. The map was reviewed by experts familiar with their particular region, including many of the original authors of the CAVM from Canada, Greenland (Denmark), Iceland, Norway (including Svalbard), Russia, and the U.S. The analysis presented here summarizes the area, geographical distribution, elevation, summer temperatures, and NDVI of the map units. The greater spatial resolution of the Raster CAVM allowed more detailed mapping of water-bodies and mountainous areas. It portrays coastal-inland gradients, and better reflects the heterogeneity of vegetation type distribution than the original CAVM. Accuracy assessment of random 1-km pixels interpreted from 6 Landsat scenes showed an

* Corresponding author.
E-mail address: mkraynolds@alaska.edu (M.K. Raynolds).

https://doi.org/10.1016/j.rse.2019.111297
Received 9 January 2019; Received in revised form 27 June 2019; Accepted 2 July 2019
Available online 17 July 2019

average of 70% accuracy, up from 39% for the original CAVM. The distribution of shrub-dominated types changed the most, with more prostrate shrub tundra mapped in mountainous areas, and less low shrub tundra in lowland areas. This improved mapping is important for quantifying existing and potential changes to land cover, a key environmental indicator for modeling and monitoring ecosystems. The final product is publicly available at www.geobotany.uaf.edu and at Mendeley Data, DOI: 10.17632/c4xj5rv6kv.1.

1. Introduction

The importance of the Arctic in relation to anthropogenic climate change has been widely recognized (IPCC, 2014), leading to increased scientific, economic and political attention. The Arctic controls large-scale atmospheric and oceanic circulation patterns, providing the cold sink for equatorial warm air masses and driving ocean thermohaline circulation (Overpeck et al., 1997). The Arctic is warming much faster than the rest of the Earth due to many factors, including the reduction in the amount and changes in the annual timing of reflective sea ice and snow (Aaron-Morrison et al., 2016; Box et al., 2019). The Arctic is also particularly vulnerable to climate warming because its ecosystems are adapted to snow and ice, which undergo abrupt transitions above freezing (Schuur et al., 2013). The melting of ocean, lake, and soil ice all cause changes in physical properties that affect climatic and biological systems (AMAP, 2017). The Arctic also hosts rich resources (both biologic and mineral), and thriving indigenous cultures (AMAP, 2018). The results of climate change will affect accessibility to resources and the way people live in the Arctic (Hoegh-Guldberg et al., 2018).

The global perspective provided by satellite views of the Earth clearly shows the Arctic as a single unit. The lands surrounding the Arctic Ocean have similar circumpolar climates and shared biologic resources. Even the governance of the area is inextricably linked, as demonstrated by the establishment and success of the international Arctic Council (Kankaanpää and Young, 2012). The Arctic Council's Circumpolar Arctic Flora and Fauna Group and other arctic researchers have long noted the need for circumpolar resource maps to be able to better understand and manage the Arctic (Walker et al., 1995). The need for land cover mapping has also been emphasized by groups such as the World Climate Research Programme (WCRP) for monitoring and implementing United Nations and European Union initiatives (Bartsch et al., 2016; Maes et al., 2012).

In response to this need, the Circumpolar Arctic Vegetation Map (CAVM) was produced in 2003 (CAVM Team, 2003). The CAVM was the first vegetation map that covered the entire Arctic using a single, unified legend. The relatively simple legend included 15 vegetation types, based largely on plant physiognomy (Walker et al., 2005). The map was a vector map, compiled from hand-drawn polygons that were interpreted using a geobotanical approach that included bioclimate subzones, floristic provinces, elevation, and substrate characteristics (Walker et al., 2002). The interpretation was done using an Advanced Very-High Resolution Radiometer (AVHRR) false-color infrared (CIR) composite base map printed at 1:4 million scale. This approach used technology that was available at the time to all the contributors from the different arctic regions (Canada, Greenland, Iceland, Norway, Russia, U.S.) (Walker et al., 2005).

Since the CAVM became available, it has been widely used by arctic researchers (Bartsch et al., 2016). It is commonly used to define the limits of the Arctic, and to locate and characterize five arctic bioclimate subzones (Walker et al., 2002). The vegetation map has been used in a range of studies, including for example, to model possible changes in arctic vegetation with climate change (Pearson et al., 2013), to stratify estimates of soil carbon (Ping et al., 2008), to study albedo (Loranty et al., 2011), to model plant migration (Hoffman, 2011), and many other applications. It has also been used to extrapolate the results of local studies to regional, continental and global scales (e.g. Blok et al., 2011). The web-site presenting the CAVM (*www.arcticatlas.org*) made the vegetation map and its themes easily available in both graphic and GIS format (including attributes for vegetation, bioclimate subzones, floristic provinces, AVHRR composite, elevation, lake cover, landscape physiography, normalized difference vegetation index (NDVI) and phytomass, substrate chemistry, and coastline). The web-site also includes detailed descriptions of the map units, with photos of the characteristic landscapes where they occur and the plant species that form the communities.

Although the CAVM provided a valuable resource as a base map for arctic studies, its vector format was not ideal for many users. In addition, with a minimal mapping unit size of 14 km diameter, the CAVM did not provide the spatial detail many researchers needed. Models commonly use satellite data for climate, elevation, etc. in a raster format. Available global raster land cover maps do not always include the whole Arctic (e.g. GLC2000, European Commission, 2003), map it with legend units not appropriate for the Arctic (such as grasslands or forests), or have relatively poor legend resolution in the Arctic, with 2 or 3 types covering the majority of the area (Bartsch et al., 2016; Krankina et al., 2011). In order to use the more appropriate legend of the CAVM, the original polygon format was often directly converted to a raster format, resulting in a relatively coarse, patchy, raster map. Researchers recognized the need for a pan-Arctic land cover map with finer spatial resolution (Bartsch et al., 2016). Current satellite data availability and advances in GIS software provide resources and tools for mapping that were not widely available in the early 2000s. The combination of emerging research needs and technological advances prompted the authors of the original CAVM to produce the Raster CAVM presented here.

2. Methods

2.1. Map extent

The Raster CAVM extent is the same as the original CAVM. It covers the Arctic, defined as the area of the Earth with tundra vegetation, an arctic climate and arctic flora, with the tree line defining the southern limit. It excludes tundra regions that lack an arctic flora, such as the boreal oceanic areas of Iceland and the Aleutian Islands, and alpine-tundra regions south of the latitudinal treeline (Walker et al., 2005).

The treeline for the original CAVM was a compilation of regional treeline maps (Walker et al., 2005). There are several projects underway to map circumpolar treeline using consistent satellite data (e.g., Montesano et al., 2016), but none of these products were available in time for this project. We therefore used the original CAVM treeline as the southern boundary of the Arctic.

We used the original CAVM coastline to delineate the seaward extent of the mapping. This coastline was based on the 1993 ESRI Digital Chart of the World (ESRI, 1993). The original coastline was simplified to match the resolution of the hand-drawn polygons, with minimum spacing between lines of 500 m, and between vertices of 5 km. All islands $< 50\ km^2$ were deleted. During the raster analysis, some details of the coastline within the CAVM extent were refined by the 1-km resolution of the classification, which separated coastal waters and lagoons from land.

We used the same projection as the original CAVM, the Lambert Azimuthal Equal Area Polar Projection.

2.2. Legend

The Raster CAVM legend uses the same units as the original CAVM (Table 1). These map units are based on the plant physiognomy of the dominant vegetation type of an area, as described on the ground by the Braun-Blanquet classification approach for plant communities (Braun-Blanquet, 1928; Walker et al., 2018) (Table S1). The legend contains five broad physiognomic categories: B = barren; G = graminoid-dominated tundra; P = prostrate dwarf-shrub dominated tundra (< 15 cm height); S = erect dwarf-shrub dominated tundra (15 to 40 cm height); and W = wetland. Barren complex map units (B2a, B2b, B3, B4) were included for areas with < 30% of any one vegetation type due to non-vegetated land cover (water, rock). The mapping units are named according to dominant plant growth forms except in the mountains where complexes of vegetation are named according to the dominant bedrock chemistry (carbonate and non-carbonate mountain complexes) (Walker et al., 2005). This is a relatively simple legend, but it has proven robust in application. Plant physiognomy units are especially relevant for mapping vegetation change and climate feedbacks in the Arctic (Pearson et al., 2013), and are more ecologically relevant than the one or two units used to map the Arctic in most global maps (Bartsch et al., 2016). One map unit, barren complex on glaciated landscapes (B2), was split into rock-water-lichen complex (B2a) and rock-water-shrub complex (B2b). A detailed legend, with descriptions of the plant species and common plant community types included in each unit is found in Table S1.

2.3. Spatial resolution

The Raster CAVM was produced at 1-km resolution. This was the resolution of the AVHRR and elevation data used in the analysis to produce the map, and thus the resolution of the classification product. The 1-km resolution is appropriate for regional to global scale maps and analyses (Walker et al., 2016). The scale matches the relatively general circumpolar legend, and is much finer resolution than many of the climate datasets used for global models. It resulted in a file size of 115 MB, an appropriate size for inclusion in many analyses. This landscape-scale resolution does not capture all the heterogeneity of tundra vegetation, but heterogeneity in the Arctic occurs all the way to sub-meter resolution (e.g., among permafrost patterned-ground features) and is only truly captured by ground sampling or the most detailed remote sensing such as LiDAR or drone imagery (Davidson et al., 2016).

2.4. Classification

The initial unsupervised classification of the CAVM was produced using Iso-cluster, a clustering procedure that iteratively groups pixels to minimize the Euclidian distance within clusters (ESRI, 2010). This is a commonly used algorithm in satellite image classification of land surface cover (e.g. Moulton et al., 2019). The Arctic was divided into 18 regions, roughly following the boundaries of the CAVM floristic provinces, based on Yurtsev (1994) (Table S2). Dividing the data set allowed the analysis to extract regional-scale variation, which was not possible when running a single classification at a circumpolar scale. Each region was classified and modeled separately, using the same seven input layers described below.

We used composited circumpolar arctic data sets as input to the analysis. The composites were created using the best available Arctic data from a number of years to get spatially consistent mid-summer values despite frequent cloud cover. Using these circumpolar composites minimized edge effects, permitting the analysis of large regions of the Arctic.

Satellite spectral reflectance data as well as vegetation indices as were used as input data, from both the AVHRR and Moderate Resolution Imaging Spectroradiometer (MODIS) sensors. In both cases, only two bands (red and near-infrared) were composited and available for this analysis. The AVHRR composite was the same image used for the initial CAVM hand-drawn mapping. The data were at 1-km resolution, compiled from US Geological Survey Global AVHRR 10-day composites from 11 July to 30 August 1993 and 1995, two unusually cloud-free summers (Markon et al., 1995). Pixels with maximum NDVI values during those periods were selected to form the composite. NDVI was calculated as: NDVI = (NIR - R)/(NIR + R), where NIR is the spectral reflectance in the AVHRR near-infrared channel (725–1100 nm, Band 2), the wavelengths where light-reflectance from

Table 1
Legend of the Raster Circumpolar Arctic Vegetation Map. See Supplemental Information for detailed legend, including plant community descriptions (SI Table 1).

Code	Unit	Description
B1	Cryptogam, herb barren	Dry to wet barren landscapes with very sparse, very low-growing plant cover. Scattered herbs, lichens, mosses and liverworts. *Zonal type in dry, continental portions of Arctic Bioclimate Subzones A and B.*.
B2a	Cryptogam, barren complex	Areas of exposed rock and lichens interspersed with lakes and graminoid areas. *Subzones C and D on the Canadian Shield.*
B2b	Cryptogam, barren, dwarf-shrub complex	Areas of exposed rock and lichens interspersed with lakes and shrubby areas. *Subzones E and D on the Canadian Shield.*
B3	Non-carbonate mountain complex	Sparse alpine vegetation and rocks on non-carbonate bedrock. The variety and size of plants decrease with elevation and latitude.
B4	Carbonate mountain complex	Sparse alpine vegetation and rocks on carbonate bedrock. The variety and size of plants decrease with elevation and latitude.
G1	Graminoid, forb, cryptogam tundra	Moist tundra with moderate to complete cover of very low-growing plants. Mostly grasses, rushes, forbs, mosses, lichens and liverworts. *Zonal type in maritime portions of Subzones A and B.*
G2	Graminoid, prostrate dwarf-shrub, forb, moss tundra	Moist to dry tundra, with open to continuous plant cover. Rushes are dominant in Subzone B and sedges in Subzone C, along with prostrate shrubs < 5 cm tall. *Zonal type in continental portions of Subzone B and C.*
G3	Non-tussock sedge, dwarf-shrub, moss tundra	Moist tundra dominated by sedges and dwarf shrubs < 40 cm tall, with well-developed moss layer. Barren patches due to frost boils and periglacial features are common. *Zonal type on nonacidic soils in Subzones D, some C and E.*
G4	Tussock-sedge, dwarf-shrub, moss tundra	Moist tundra, dominated by tussock cottongrass (*Eriophorum vaginatum*) and dwarf shrubs < 40 cm tall. Mosses are abundant. *Zonal type on acidic soils in Subzone E, some D.*
P1	Prostrate dwarf-shrub, herb, lichen tundra	Dry tundra with patchy vegetation. Prostrate shrubs < 5 cm tall (such as *Dryas* spp. and *Salix arctica*) are dominant, with graminoids and forbs. Lichens are also common. *Zonal type in dry, continental portions of Subzones B and C, and at higher elevations in Subzones D and E.*
P2	Prostrate/hemi-prostrate dwarf-shrub, lichen tundra	Moist to dry tundra dominated by prostrate and hemiprostrate shrubs < 15 cm tall, particularly *Cassiope* spp. *Zonal type in maritime, acidic portions of Subzone C.*
S1	Erect dwarf-shrub, moss tundra	Tundra dominated by erect dwarf-shrubs, mostly < 40 cm tall. *Zonal type in continental areas with acidic soils of Subzone D.*
S2	Low-shrub, moss tundra	Tundra dominated by low shrubs > 40 cm tall. *Zonal type in warmer, maritime portions of Subzone E, and in areas with deep, moist active layers.*
W1	Sedge/grass, moss wetland complex	Wetland complexes in the colder areas of the Arctic, dominated by sedges, grasses and mosses. *Subzones B and C.*
W2	Sedge, moss, dwarf-shrub wetland complex	Wetland complexes in the milder areas of the Arctic, dominated by sedges and mosses, but including erect dwarf-shrubs < 40 cm tall. *Subzone D.*
W3	Sedge, moss, low-shrub wetland complex	Wetland complexes in the warmer areas of the Arctic, dominated by sedges and shrubs > 40 cm tall. *Subzone E.*

the plant canopy is maximal, and R is the reflectance in the red channel (580–680 nm, Band 1), the wavelengths of maximum chlorophyll absorption. AVHRR Band 1, Band 2 and NDVI were the three layers produced in this composite, and all three were used as input layers in the unsupervised classification.

Three similar data layers were used from the MODIS circumpolar composite: Band 1 (red; 620–670 nm), Band 2 (NIR; 841–876 nm), and NDVI. The addition of the MODIS data strengthened the analysis by providing an independent measure of NDVI from a different sensor and later time period. The MODIS composite was produced by the Canadian Centre for Remote Sensing for the circumboreal region and depicts the maximum NDVI value for each pixel from a 10-day, mid-summer compositing window for the years 2000–2009 (Trishchenko et al., 2009). The composite was produced using adaptive regression and normalization to preserve the image radiometric properties, and included a cloud and cloud shadow detection method, and a clear-sky compositing scheme. This product was produced at 250-m spatial resolution. However, the raster classification technique produced results at the resolution of the coarsest input layer, so in order to have the MODIS data equally weighted, they were degraded to 1-km resolution for this analysis using a bilinear resampling technique. The three available layers, Band 1, Band 2 and NDVI were used as inputs.

The seventh layer input to the classification analysis was 1-km resolution elevation data from the Digital Chart of the World (ESRI, 1993). We tried including temperature and precipitation data in the classification analysis, but the data were not available at a fine enough spatial resolution for the entire circumpolar area. Their inclusion in the unsupervised classification resulted in unacceptably blocky patterns reflecting their coarse spatial resolution (25 km or larger pixels). These data were, however, used as ancillary data after the initial classification (see below).

All data layers needed to have same range of values so as not to over- or under-weight any one layer. All seven input layers were indexed from 0 to 1000 using the following scaling equation and the range of values within each analysis region:

$$Z = \frac{(\mathrm{X}-\mathrm{oldmin}) \times (\mathrm{newmax}\text{-}\mathrm{newmin})}{(\mathrm{oldmax} - \mathrm{oldmin})} + \mathrm{newmin}$$

The maximum suggested number of classes for the clustering analysis was 10 times the number of input layers (70), and approximately 5 times the number of final units desired. The analysis was run for 50 classes for the most diverse regions close to treeline, and 20 classes for the least diverse regions in the High Arctic. The minimum class size was set to approximately 1% of a region (most commonly 500 pixels, ranging from 100 to 1000 pixels). The sampling interval was set to 1 pixel (i.e. all pixels were included in the analysis). The number of iterations was set to 20 (the default).

The groups produced by the unsupervised classification were modeled to the CAVM legend units using a variety of ancillary data. This approach using unsupervised classification and modeling has been found to produce better results than supervised classification of tundra vegetation (Joria and Jorgenson, 1996). For example, Latifovic et al. (2017) in creating a Landsat classification of the Canadian North first used unsupervised classification to create their training data for classifying the rest of the tiles using Random Forest. The unsupervised classification results were good enough to use as training data, but this method could not be applied to the whole area at the Landsat scale because interpreting the results of the unsupervised classification "… requires considerable time, expertise in image interpretation, and knowledge of the land cover in the area of interest." (Latifovic et al., 2017). This project was able to use this approach for the entire map, because of the coarser spatial resolution of the map (1 km vs Landsat 30 m pixels) and the participation of regional arctic vegetation mapping experts for every portion of the map.

The classification units were compared with ancillary data layers to assign each unit to a preliminary CAVM vegetation unit. Regional vegetation maps were the most important resources for this step, and were available for Alaska, parts of Canada, Greenland and Russia. Landsat-scale (30-m resolution) land cover maps were available for Alaska, northern Canada, Iceland and Svalbard. Ground studies and vegetation descriptions were consulted for all sections of the map. High resolution imagery hosted on Google Earth and the ground photos posted on Google Earth were especially helpful for areas with limited ground data. In cases where one classification unit included more than one CAVM legend unit, cut-point equations were developed to split the unit. For example, in some cases MODIS Band 2 data were used to identify and re-assign water pixels within a unit. Geology maps were used to differentiate between acidic and nonacidic mountain units. Elevation data were used to identify areas over 1000 m elevation, where adiabatic cooling would result in a significantly cooler climate than at sea level, resulting in a different bioclimate subzone and different vegetation than the surrounding areas at lower elevations. Climate data, including locally available ground data and interpolated data, were used as ancillary layers. See Table S3 for a list of ancillary data sources for each portion of the map.

2.5. Review

Each portion of the draft map was sent to experts with experience mapping the vegetation of that particular area. The input from these reviewers was used to improve the map and the legend description of plant communities included in each mapping unit.

The final review was a consistency check to ensure that the map units were consistently interpreted throughout the circumpolar extent. The NDVI values and Summer Warmth Index (SWI, the sum of monthly mean temperatures above 0 °C) were evaluated within each unit to identify any outlier areas. These areas were then examined using ancillary data and reviewer input, and re-mapped if necessary.

2.6. Accuracy assessment

Landsat 8 Operational Land Imager (OLI) scenes were selected in six widely distributed areas where the primary authors had personal ground experience: North Slope and Seward Peninsula, Alaska; Kolyma River, Yakutia; Yamal Peninsula, European Russian Arctic; Baffin Island, Nunavut; and Ellef Ringnes Island, Nunavut. The most recent available scenes with cloud-free summer coverage were selected using the USGS GloVis web site (2016–2018, Table S4). A random raster with values from 0 to 1 was created with the same pixel size and projection as the Raster CAVM, and the same extent as each Landsat scene. Approximately 100 random 1-km pixels were selected in each scene. Selecting random pixels with values < 0.003 resulted in approximately the right number of pixels for most scenes, though some scenes needed more pixels because of areas excluded due to ocean or clouds.

The dominant CAVM unit within each selected 1×1 km pixel was determined by visual interpretation from a CIR rendering of the Landsat data, and compared with the Raster CAVM mapping and the original vector CAVM mapping. The accuracy of map units within each Landsat scene was calculated from these random points, and the accuracy of the six scenes averaged to estimate the overall Raster CAVM accuracy. For each scene, additional pixels were selected within rare vegetation types that had at least 100 pixels (approximately 0.25% of area). The accuracies from these rare-type pixels were used to evaluate the mapping of particular units in particular scenes, but not included in the overall accuracy assessment summary.

2.7. Analysis

We summarized the total area of the different map units and the area of each unit in different countries. We compared the area and proportions of the different map units in the original CAVM and the Raster CAVM. We tabulated the area of each map unit within each

country, and within each bioclimate subzone.

For each vegetation type, we calculated the average elevation based on the 1-km resolution elevation data from the Digital Chart of the World (ESRI, 1993), bioclimate subzone based on AVHRR surface temperature data 1982–2003 (Raynolds et al., 2008a), and NDVI values based on AVHRR and MODIS composites (Markon et al., 1995; Trishchenko et al., 2009). We compared the Raster CAVM to a rasterized version of the original vector CAVM to identify which pixels had changed and summarized that information by map unit.

The relationship of the Raster CAVM mapping to temperature was analyzed used SWI based on AVHRR land surface temperature 1982–2003 (Raynolds et al., 2008a). The temperature data were 12.5-km resolution, so they could not capture landscape-scale gradients that can be prominent at smaller scales in the vegetation map (e.g., mountainous areas and coastal areas), but were adequate to show general patterns of correspondence with the map units.

3. Results

The total area of the Arctic as shown on the Raster CAVM (Fig. 1) was 7.02×10^6 km^2, with about 46% of the area covered by vegetated map units (about 3.24×10^6 km^2) (see Table S5 for area summaries). The remainder was ice covered (29%), barren (21%), or fresh water (4%). About 47% of the vegetated portion of the Arctic was shrub-dominated, 45% was graminoid-dominated, and 8% was wetlands. The non-ocean area of the Arctic as shown on the Raster CAVM was slightly smaller than that of the original CAVM (7.1×10^6 km^2) because of the areas of saline lagoons and coastal inlets (0.08×10^6 km^2), that were defined and excluded using the finer-resolution Raster CAVM.

The area of each map unit in each country is shown in Fig. 2 (values in Table S5). Canada had by far the most terrain in barren types, with high cover of cryptogam barrens (map unit B1) throughout the Canadian Arctic Archipelago. Many continental portions of the Canadian Shield were also covered with barren complex vegetation, especially B2a. Russia had more mountain complex area (especially, non-carbonate mountain complex, B3) than other countries. Russia also had more cover of graminoid units, including both non-tussock graminoid tundra (G3) found in the western Russian Arctic, and tussock tundra (G4) in eastern Siberia and Chukotka. Shrub types were most common in Canada and Russia. In Canada, the prostrate shrub unit (P1) was especially common on Victoria Island and other parts of the western Canadian Arctic Archipelago. Russia had more erect dwarf-shrub tundra (S1), which occurred throughout the southern parts of the Russian Arctic. Wetlands (W1–3) were most common in Russia and the U.S. Large deltas, such as those of the Lena and Yukon Rivers were locations with extensive wetlands.

While generally showing similar distributions of arctic vegetation types, a comparison of a rasterized version of the original CAVM and the new Raster CAVM showed only 31% overall agreement on a pixel-by-pixel basis (Table S6). Fig. 3 highlights some important differences (values in Table S5). Due to the finer pixel resolution, the Raster CAVM mapped over four times as much area of fresh water as the vector CAVM, including many small ponds, as seen in Fig. 1 (bottom). 84% of the area that was mapped as fresh water in the original CAVM was

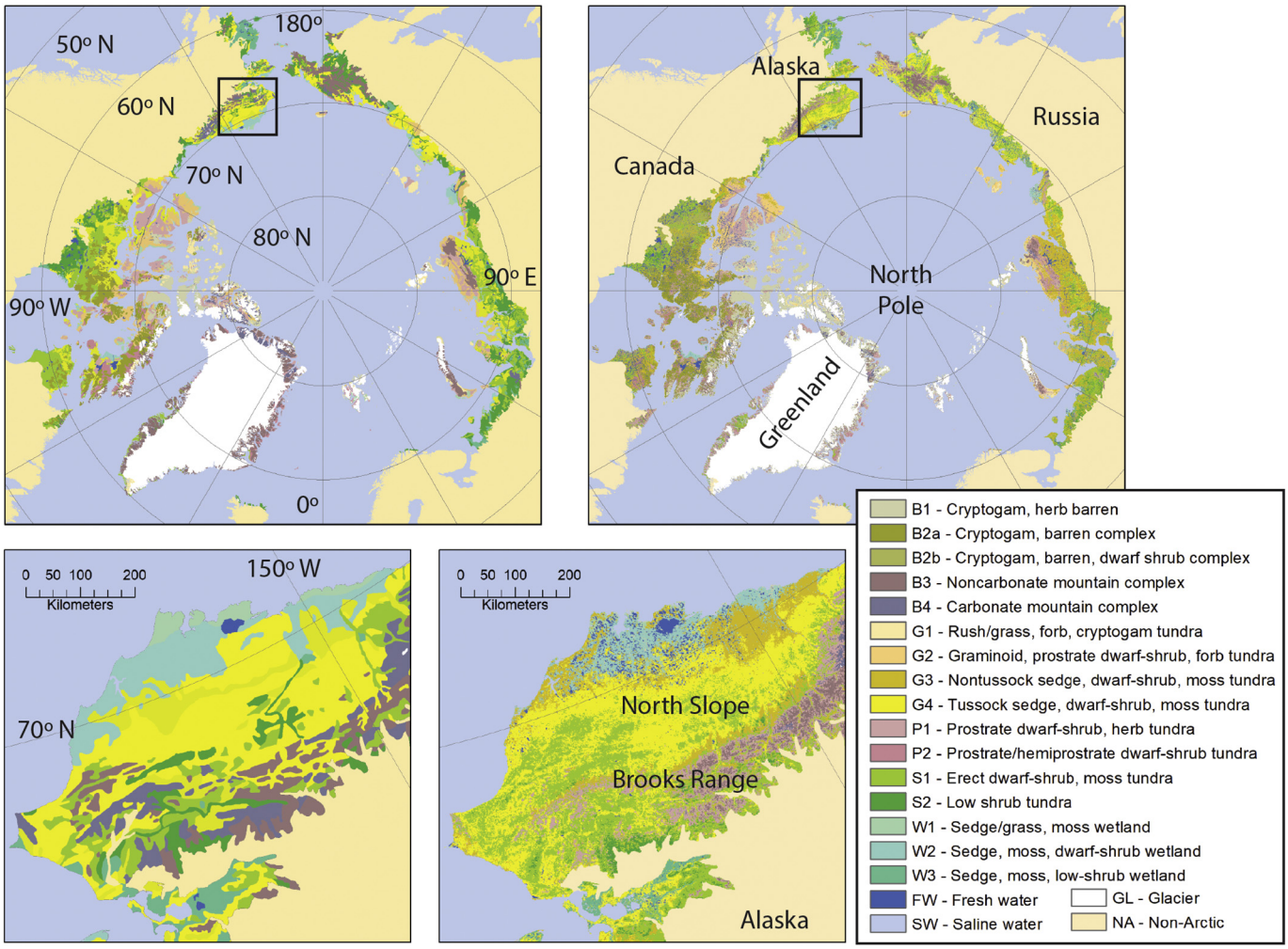

Fig. 1. Comparison of the original vector CAVM (top left) and new Raster CAVM (top right), and zoom in to northern Alaska (vector bottom left, raster bottom right).

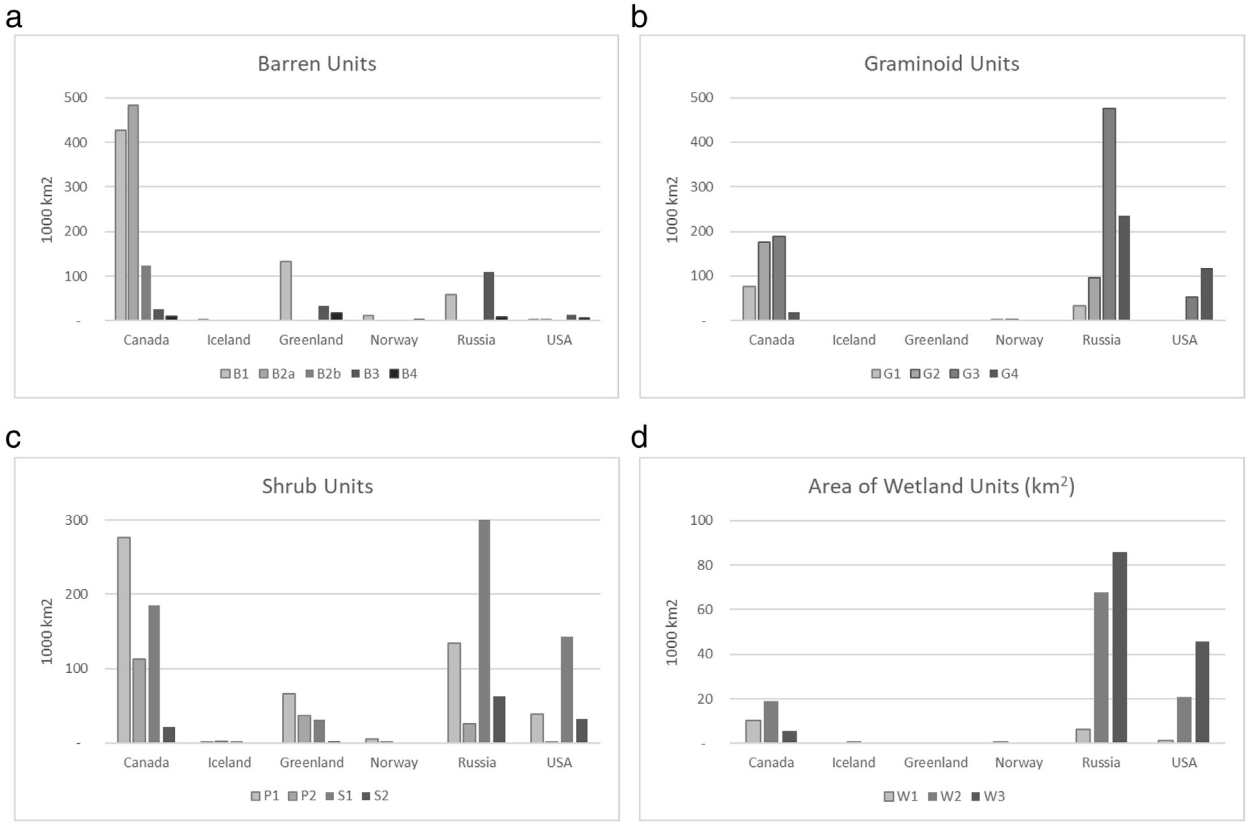

Fig. 2. Area of different types of plant cover (a) barren, b) graminoid, c) shrub, d) wetland) within the arctic portion of six countries, as shown on the Raster CAVM. Map units are ordered from colder to warmer (left to right). Norway includes Svalbard and a small portion of northern Norway (Finnmark). Note differing vertical scales.

mapped as fresh water in the Raster CAVM, and additional water pixels were most commonly from areas formerly mapped as shrub (Table S6). There was more barren (B1) shown in the Raster CAVM, mostly drawn from mountain complex types (B3 and B4) that could be mapped in more detail with the raster version's 1-km resolution. Similarly, the Raster CAVM showed more prostrate shrub (P1), which mostly came from mountain complexes. The Raster CAVM also showed more area of the bedrock complexes of the Canadian Shield (B2a and B2b), with less of this area mapped as either graminoid or shrub cover, due to incorporating improved local maps for the Canadian Shield (Latifovic et al., 2017) and other sources (Table S3). The Raster CAVM showed less than one-fifth the area of low-shrub tundra (S2) as the original vector version of the map, with most of this area mapped as erect dwarf-shrub tundra (S1). This change was due to better ground data and local vegetation maps for Russia and Canada (Table S3).

Patterns of correspondence between the map units and NDVI were strong and generally conformed to expectations (Fig. 4) (Raynolds et al., 2006). NDVI values were greatest for those map units found farthest south, which is not surprising, as NDVI is a proxy for vegetation biomass and productivity, which increase with summer temperatures in the Arctic (Epstein et al., 2008). This was the case with NDVI from both MODIS and AVHRR sensors, whose means and variability for different

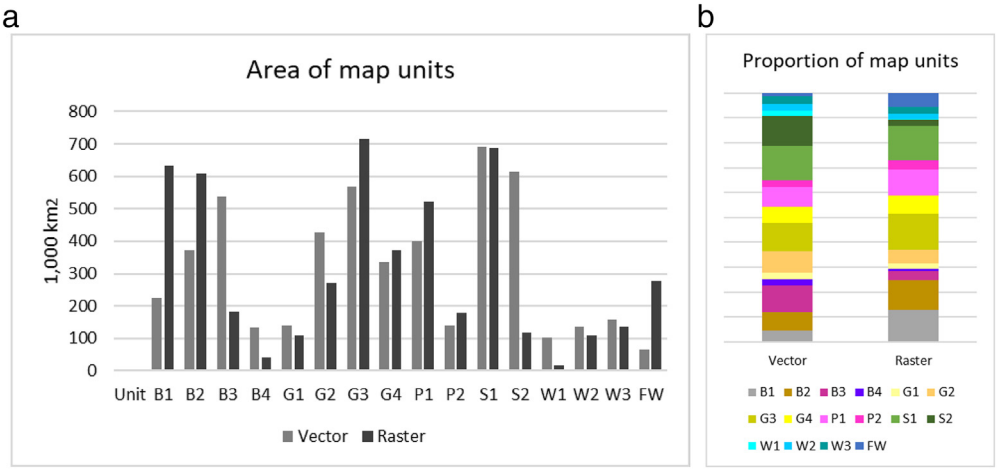

Fig. 3. a) Comparison of area of different map units on the vector CAVM (left, light-gray bars) and the Raster CAVM (right, darker bars). b) Proportions of different map units on the vector CAVM (left) and the Raster CAVM (right). B2a and B2b in the Raster CAVM are combined for this comparison.

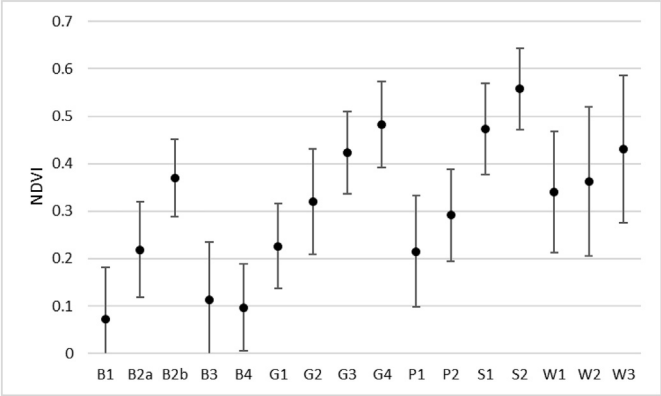

Fig. 4. NDVI of each map unit on the Raster CAVM (mean ± s.d.), from MODIS data set (Trishchenko et al., 2009).

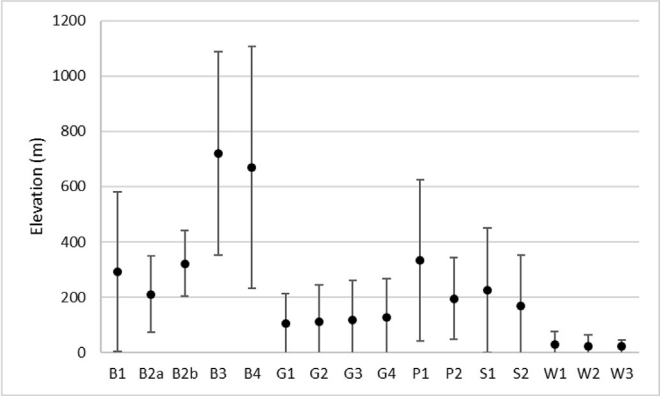

Fig. 5. Elevation (AMSL) (ESRI, 1993) of each map unit on the Raster CAVM (mean ± s.d.).

map units were very similar (linear regression fit of mean map unit NDVI AVHRR vs. MODIS, $R^2 = 0.99$). Most of the area with NDVI < 0.2 was the barren map unit (B1) (Table 2). From NDVI 0.2 to 0.3, rock-lichen complex (B2a) and prostrate shrub tundra (P1) were common. Between 0.3 and 0.4, graminoid-erect dwarf-shrub tundra (G3) was most common. Between 0.4 and 0.5, types with erect dwarf-shrubs (G3 and S1) were the most common. Between 0.5 and 0.6, erect dwarf-shrub tundra (S1) was most common. Most of the areas with NDVI > 0.6 were mapped as erect- and low-shrub types (S1 and S2).

Average elevation of different map units showed the mountain-complex types (B3, B4) with the highest elevations and greatest variability (Fig. 5). The prostrate shrub type (P1), which is found in alpine areas, also had a relatively high average elevation. Wetland types (W1–3) had the lowest elevations and lowest variability. Most of the Arctic is < 500 m elevation, with the lowest elevations (< 100 m) dominated by graminoid-erect dwarf-shrub tundra (G3) (Table 3). The most common map unit at elevations over 1000 m were the mountain complexes (B3 and B4) and the prostrate dwarf-shrub type (P1).

The relationship of the Raster CAVM mapping to SWI (Fig. 6), was similar to NDVI patterns (Fig. 4) even though temperature was not included in the classification. This is not surprising, as vegetation biomass and productivity in the Arctic are usually closely linked to summer temperatures (Epstein et al., 2008). The circumpolar summaries showed expected patterns, with the barren map unit (B1) found in the coldest part of the Arctic, and the barren-lichen complex (B2a) in colder areas than the barren-shrub complex (B2b) on the Canadian Shield. The average temperature of the graminoid-dominated types varied with species composition, with the rush/grass type (G1) colder than the graminoid-prostrate shrub type (G2), which was colder than the graminoid-erect dwarf-shrub type (G3), which was colder than the tussock-shrub type (G4). The shrub types followed a similar pattern: the prostrate-shrub type (P1) the coldest, followed by the hemiprostrate-shrub

Table 3
Area (1000 s of km^2) of different Raster CAVM map units in different elevation categories (based on ESRI elevation data). Total area excludes lakes, glaciers, and ice caps.

Map unit	< 100 m	100–499 m	500–999 m	1000–1499 m	≥1500 m
B1	192	305	125	11	4
B2a	100	367	17	0	0
B2b	1	114	10	0	0
B3	2	52	98	24	9
B4	2	15	16	6	3
G1	65	43	1	0	0
G2	168	94	11	0	0
G3	450	246	19	0	0
G4	218	141	13	0	0
P1	100	312	89	21	2
P2	49	122	8	0	0
S1	275	332	74	7	0
S2	51	59	7	0	0
W1	17	1	0	0	0
W2	105	4	0	0	0
W3	136	2	0	0	0
Total land area	1929	2211	488	70	17
Lakes	150	119	9	0	0
Glaciers & ice caps	42	122	261	298	1324

Table 2
Area (1000 s of km^2) of different Raster CAVM map units in different MODIS NDVI categories. Glaciers, ice caps and lakes are not included.

Vegetation type	< 0.2	0.2–0.29	0.3–0.39	0.4–0.49	0.5–0.59	0.6–0.69	≥0.7
B1	601	25	6	4	1	0	0
B2a	188	201	85	11	0	0	0
B2b	3	15	61	42	3	0	0
B3	147	20	11	5	1	0	0
B4	37	3	1	0	0	0	0
G1	37	53	17	2	0	0	0
G2	27	89	90	61	6	0	0
G3	13	38	182	378	100	4	0
G4	6	7	26	163	164	7	0
P1	239	183	63	32	7	0	0
P2	21	70	71	17	1	0	0
S1	12	21	88	281	251	34	1
S2	1	1	3	24	56	31	3
W1	2	3	7	5	1	0	0
W2	11	11	35	42	10	0	0
W3	9	8	22	50	45	4	0
Total	1351	749	768	1116	647	80	4

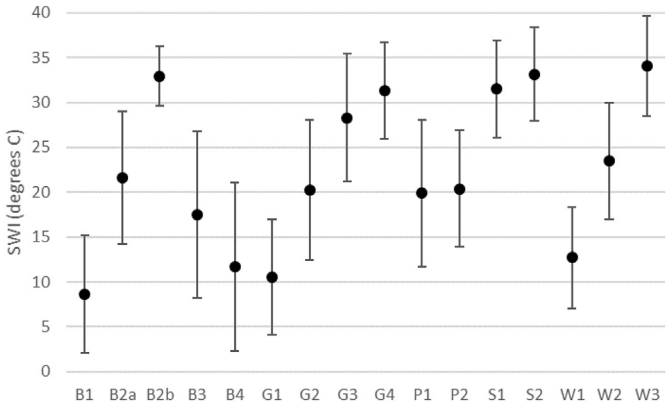

Fig. 6. Summer Warmth Index (SWI) of each map unit on the Raster CAVM (mean ± s.d.). SWI is calculated as the sum of annual monthly means above 0 °C, based on AVHRR surface temperature 1982–2003 (Raynolds et al., 2008a).

(P2), the erect dwarf-shrub (S1) and the low-shrub type (S2). The coldest wetland type had few shrubs (W1), the next warmest (W2) had dwarf shrubs, and the warmest (W3) had low shrubs.

The SWI data were grouped to represent the five bioclimate subzones of the Arctic, A through E (colder to warmer) (Raynolds et al., 2008a). Map unit B1 is the only type that occurred mostly in the coldest subzones A and B (Table 4). The barren complex units occurred mostly in subzones C, D (B2a) and E (B2b). G1 occurred predominantly in Subzone B, G2 in subzones C and D, G3 in Subzone D, and G4 in subzones D and E. P1 occurred in all subzones, but as a zonal low-elevation type in Subzone B, and at higher elevations in warmer subzones. P2 was most common in subzones C and D, S1 in subzones D and E, and S2 in subzone E. W1 was most common in subzones B and C, W2 in subzone D, and W3 in subzone E. The occurrence of some W3 pixels in subzones B and C was due to the large size of the SWI pixels (12.5 km), so a temperature pixel dominated by cold ocean might extend inland, where in actuality warmer temperatures and corresponding vegetation occur on the ground. Mountain types (B3, B4) occurred in all subzones, except in the warmest subzone, E. This is because any mountains occurring along the southern boundary of the Arctic (e.g. Alaska Brooks Range) are cooler than the surrounding lower elevations which are in subzone E. If the mountains themselves were warm enough to be subzone E, the surroundings areas would be even warmer and boreal, and the mountains would be mapped as alpine boreal rather than arctic (e.g., the Canadian Rocky Mountains).

The only map unit whose mean NDVI did not match the pattern of the mean SWI was the rush/grass unit (G1). This type had colder temperatures than the mountain units, but a higher NDVI value than is typical of mountains. This is likely due to the fact that G1 is mostly a coastal type, occurring in cold areas, but on relatively nutrient-rich sediments.

The accuracy of mapping within the six Landsat scenes varied from 57% to 90% (average 70%, Table 5). The most accurately mapped scenes were areas with few, relatively homogeneous vegetation types (e.g. Ellef Ringnes Island, 90%). Conversely, the least accurate scenes were areas with many types (Kolyma, 57% and Seward, 59%) and scenes with many mixed-pixels, such as the highly dissected Yamal Peninsula (67%). The results for each Landsat scene are included in the Supplementary Materials (Tables S7–S12), and include pixels of the relatively rare map units in each scene.

Highest accuracies were found for map units that occurred in relatively large uniform areas or complexes (e.g. barren and mountainous types, B1-B4, 67–100% accuracy) and water, with its distinctive spectral signature (69–71%) (Table 5). Lowest accuracies were for uncommon types (graminoid tundra in subzones A and B, G1-G2, 11–100% and low shrub, S2, 43–62%). The most commonly confused type was erect dwarf shrub tundra (S1). Many of the pixels that were mapped as S1 were interpreted as graminoid tundra (G4 in S1 row, Table 5), and similarly, many of the pixels that were interpreted as S1 were mapped as graminoid tundra (G3, G4 in S1 column, Table 5).

4. Discussion

The Raster CAVM combined the advantages of both the original CAVM and the raster format. The advantages of the original CAVM that were retained included the easily understood, ecologically relevant circumpolar legend based on plant physiognomy; the equal area polar projection (Lambert Azimuthal); and the previously agreed-upon Arctic boundaries (especially treeline). The Raster CAVM mapped the whole Arctic biome, using a consistent legend, a consistent method and consistent data sources (AVHRR and MODIS satellite data and elevation). The advantages of the raster format included the ability to incorporate information from recent mapping efforts based on Landsat and other mid-resolution satellite data, the vastly improved spatial resolution, and the compatibility of the final product with satellite and climate data sets used for modeling and other studies.

Overall, the Raster CAVM showed a similar distribution of vegetation types as the original vector CAVM (Fig. 1, top). Major global biogeographic patterns were mapped, such as the north-south gradient in vegetation types, and east-west patterns such as the predominance of tussock tundra (G4) throughout Beringia. The greater spatial resolution of the Raster CAVM, and its ability to show landscape-scale variation within the original CAVM polygons is striking (Fig. 1, bottom). For example, the much more detailed representation of waterbodies in lake-rich regions such as Alaska's North Slope demonstrated the ability of the Raster CAVM to map units with scattered, small extents. Similarly, the mapping of the Brooks Range Mountains showed how the finer spatial resolution made it possible to map intermontane valleys and lower slopes within the mountains. The mapping of these areas using low-shrub tundra (S1), prostrate-shrub tundra (P1), and barren (B1) provided much more information than the previous mapping, where montane areas could only be mapped as complex units (B3 and B4).

4.1. Raster CAVM extent

We considered revising the CAVM treeline as part of the process of making the Raster CAVM. We recognized that better mapping was available for some areas than was used for the original CAVM and that

Table 4
Area (1000 s of km^2) of different Raster CAVM map units in each bioclimate subzone. Subzones based on binned AVHRR SWI (° C) (Raynolds et al., 2008a); A = 0.1–5, B = 5–14, C = 14–22, D = 22–32, E = 32–45). Total land area excludes lakes, glaciers, and ice caps.

Map unit	A	B	C	D	E
B1	230	267	103	24	3
B2a	12	61	185	205	37
B2b	0	1	2	39	89
B3	29	39	50	63	6
B4	13	10	12	5	1
G1	25	50	26	7	0
G2	9	52	90	103	20
G3	1	33	89	361	242
G4	0	6	11	187	171
P1	25	104	174	194	32
P2	3	27	76	73	5
S1	0	8	38	305	355
S2	0	1	6	39	76
W1	1	9	6	2	0
W2	0	13	20	73	5
W3	0	1	3	38	96
Total land area	347	681	891	1717	1138
Lakes	5	18	63	139	60
Glaciers & ice caps	381	124	3	0	0

Table 5
Accuracy assessment "confusion" matrix, showing the correspondence between the Raster CAVM mapped units (rows) and the Landsat scene 1-km pixel interpretations (columns). Six selected Landsat 8 OLI scenes were sampled, with approximately 100 points each. The number of pixels for which the mapping matched the interpretation are in bold, forming a diagonal line. The number in the lower right corner is the overall accuracy (70%).

	Landsat interpretation															
Raster CAVM	B1	B2	B3	B4	G1	G2	G3	G4	P1	P2	S1	S2	W2	W3	WA	User's accuracy
B1	**97**	1	0	0	8	0	1	0	0	0	0	0	1	3	1	**0.87**
B2	2	**27**	0	0	0	0	0	1	10	0	0	0	0	0	0	**0.68**
B3	0	0	**5**	0	0	0	0	0	0	0	0	0	0	0	0	**1.00**
B4	0	0	0	**4**	0	0	0	0	0	0	0	0	0	0	0	**1.00**
G1	0	0	0	0	**1**	0	0	0	0	0	0	0	0	0	0	**1.00**
G2	1	0	0	0	0	**7**	0	0	0	0	0	0	0	2	0	**0.70**
G3	0	0	0	0	0	1	**59**	8	4	0	18	0	4	10	1	**0.56**
G4	0	0	0	0	0	0	5	**55**	0	0	16	2	4	1	1	**0.65**
P1	4	6	0	2	0	0	0	0	**41**	0	1	0	0	2	0	**0.73**
P2	0	0	0	0	0	0	0	0	2	**9**	0	0	0	0	0	**0.82**
S1	0	0	0	0	0	0	3	11	7	1	**39**	0	1	1	0	**0.62**
S2	0	0	0	0	0	0	0	0	0	0	4	**3**	0	0	0	**0.43**
W2	1	0	0	0	0	0	0	0	0	0	0	0	**21**	0	1	**0.91**
W3	0	0	0	0	0	4	4	2	0	0	0	0	0	**32**	6	**0.67**
WA	1	1	0	0	0	0	0	0	1	0	1	0	1	6	**24**	**0.69**
Producer's accuracy	**0.92**	**0.77**	**1.00**	**0.67**	**0.11**	**0.58**	**0.82**	**0.71**	**0.63**	**0.90**	**0.49**	**0.60**	**0.66**	**0.56**	**0.71**	**0.70**

in some areas treeline location may have changed since the regional maps that were used for the CAVM treeline were drawn. However, we were not able to find consistent, updated treeline data. There was a revised version of the Alaska treeline, delineated as part of the Circumpolar Boreal Vegetation Map project (Jorgenson and Meidinger, 2015). However, similar products were not available for Canada or Russia.

Areas of contention included the Kola Peninsula in western Russia, which the original CAVM excluded. Parts of the northern Kola Peninsula, near the Barents Sea, would likely be included within the Arctic, following a consistent circumpolar treeline definition (Koroleva, 1994). The area south of the Anadyr River in eastern Russia, which the original CAVM included, would likely be excluded due to the widespread occurrence of dwarf Siberian pine (*Pinus pumila*), growing there (V. Razzhivin, pers. comm.). Mountainous areas such as northern Alaska's Brooks Range, the mountains south of the Taimyr Peninsula, and Yakutia's Verkhoyansk Mountains should be treated consistently. If trees grow in these areas at low elevations, the areas above altitudinal treeline should be mapped as part of the Boreal Alpine, not the Arctic.

An updated coastline could have included smaller islands, and also have captured any changes resulting from coastal aggradation and erosion (e.g., Pfalz, 2017). We chose to retain the original CAVM coastline, as the purpose of making this Raster CAVM was not to map change, but rather to provide a comparable raster version of the original CAVM. Similarly, we used the original CAVM Greenland Ice Cap extent, though this has also changed. Retaining the original CAVM extent ensured that researchers who used the original CAVM to define their study areas would not have to revise them in order to use the digital map.

A complete review of the extent of the Arctic land area is an important future project. The Raster CAVM used the existing CAVM extent boundaries, partly to make the updated map more compatible with the previous map, and partly because of the difficulty of delineating a new set of boundaries from partial datasets. NASA is working on a circumpolar Landsat-based tundra-taiga ecotone product (Montesano et al., 2016). It describes a gradient of boreal forest cover, is based on Landsat 30-m resolution tree cover data, and is calibrated using finer resolution QuickBird data for areas throughout the Arctic and also uses North American LiDAR data. It is expected to be publicly available in 2019, likely as an asset in Google Earth Engine (P. Monsanto pers. comm.). This will be a valuable resource for any studies related to the forest-tundra transition, and can be used to develop a much more appropriate arctic boundary than the current CAVM treeline.

NASA has also produced arctic coastline and glacier boundaries (EASE-Grid 2.0 Land-Ocean-Coastline-Ice Masks derived from Boston University MODIS/Terra Land Cover Data, Version 1), hosted by the National Snow and Ice Data Center (NSIDC) that could be used to update ocean and glacier boundaries. These products, once checked to ensure georegistration between the layers, could be used to update the extent of the Arctic as mapped by the Raster CAVM.

4.2. Raster CAVM legend

The original CAVM, with its 14-km minimum polygon size, was acknowledged as a map that included a great deal of heterogeneity within the mapped polygons. The goal was to map the zonal vegetation within a polygon, defined as the vegetation that develops over time on mesic soils in balance with the local climate (Walker et al., 2005). This definition excluded areas with extremes of slope, soil chemistry or moisture. However, it was recognized that within a mapped polygon, a range of topographic positions existed, including ridges, snowbeds, and riparian areas that could support non-zonal vegetation. This is especially true in the southern Arctic, where a greater number of vascular plant species exist that can grow together to form a variety of communities. By focusing on the zonal vegetation, while acknowledging this within-polygon diversity, the original CAVM effectively conveyed the general distribution of arctic vegetation.

The CAVM legend, though comprehensive and applicable for many uses, does have some drawbacks. By focusing on the physiognomy of vascular plants, the legend does not directly address non-vascular plants. Many of the vascular plant communities have characteristic non-vascular associates (see detailed legend, Table S1). However, there are variations in the non-vascular communities that are ecologically important and not separated in the CAVM legend. The thickness of the moss and lichen layer is particularly important in modeling the insulating effects of vegetation on soils, and thus important for permafrost and carbon modeling (Bartsch et al., 2016). It may be possible to map these nonvascular communities in more detail by incorporating other types of remote sensing indices and/or radar or LiDAR. Quantitative/continuous field maps of vegetation canopy height, cover of plant functional types, and other products could be used to improve the legend in specific regions, as those products are developed.

Similarly, the height of tundra shrubs is important for modeling the effects on snow, due to both snow trapping during winter and reduced albedo during snowmelt (Sturm et al., 2005). The CAVM legend includes three shrub-dominated map units, characterized by height

(prostrate shrubs: < 15 cm, erect dwarf-shrubs: 15–40 cm, and low shrubs: > 40 cm). Additional information on shrub height could be extracted from radar remote sensing (Bartsch et al., 2016), stereo photogrammetric approaches (Montesano et al., 2017), or from seasonal remote sensing images that show snow accumulation and melt patterns (Macander et al., 2015).

4.3. Raster CAVM resolution

The ideal scale for mapping tundra vegetation depends largely on the purposes of the map (Marceau, 1999). The Raster CAVM, with its 1-km pixel resolution, was able to come closer to mapping the actual vegetation on the ground than the original CAVM. However, since the classification was done using satellite data, it is based on the average reflectance of each 1-km pixel area. Especially in the Arctic, one square kilometer still includes significant vegetation heterogeneity. Even at a sub-meter scale, differences in micro-elevation relate closely to substrate moisture and variation in vegetation that can be mapped in tundra landscapes (Raynolds et al., 2008b).

Recent research has shown that even imagery as fine as 2-m resolution may not be adequate to map important variation in tundra vegetation for some purposes. Virtanen and Ek (2014) found that finer resolution imagery increased the accuracy of their mapping, in a study that used Landsat TM5 30-m, Aster 15-m, and QuickBird 2.4-m resolution imagery. Interestingly, the overall proportions of the vegetation types in their study area in north-eastern European Russia did not differ much with scale, implying a fractal nature to the distribution of vegetation in that area. Davidson et al. (2016) found that 2-m Worldview data was too coarse to adequately map the vegetation within eddy covariance tower footprints near Utqiagvik, Alaska (formerly Barrow). Langford et al. (2016) successfully mapped plant functional types in this area using a seasonal cycle of 2-m Worldview data in combination with LiDAR data. Recent neural network analysis of sub-meter imagery successfully produced maps of ice-wedge polygons near Nuiqsut in northern Alaska (Zhang et al., 2018), which could be used to map the characteristic vegetation that occurs on the rims, troughs and centers of the polygons.

Finer-resolution maps are particularly effective in classifying small water-bodies. This is exemplified by the 4× increase in water cover shown on the Raster CAVM compared to the original CAVM. Finer resolution mapping of water and wetlands has been shown to have significant effects on the results of carbon models (Treat et al., 2018). Additional work to extract more information from the 1-km Raster CAVM could be done by combining with finer-resolution remote sensing or existing hydrographic datasets. Spectral unmixing methods can be used to make maps of the fractional cover of different vegetation types within a pixel (Macander et al., 2017; Olthof and Fraser, 2007; Zhang and Li, 2012). Statistical models and probability maps indicating the presence and abundance of vegetation types or plant species can be built by combining field data with reflectance data (Brossard and Joly, 1994; Takeuchi et al., 2003). Including radar data can also improve the resolution of vegetation mapping (Bartsch et al., 2016).

At this point in time, it is not feasible to map the entire Arctic at under 30-m resolution. The quality and coverage of available imagery is relatively poor because high-resolution satellites are relatively recent, their imagery is expensive to acquire, and Arctic regions experience frequent cloudiness and a short snow-free season resulting in small acquisition windows. Mapping the Arctic at 30-m resolution (e.g. Landsat) would map more detail, but would not fully resolve the issue of heterogeneous vegetation, would have the disadvantages of a much larger dataset and its attendant storage and computational limitations, and would have greater compatibility issues between scenes (e.g. edge artifacts) due to long return times and prevalent cloud cover in the Arctic. As the remote sensing image libraries improve, there is potential for using Google Earth Engine and other cloud-based computing to carry out the data intensive processing necessary to produce a circumpolar classification at finer resolution than 1 km. In the meantime, the 1-km scale of the Raster CAVM provides an ecologically relevant resolution compatible with many other circumpolar data sets.

4.4. Accuracy assessment

The overall accuracy estimate for the Raster CAVM of 70% was a large increase in accuracy from the original CAVM, whose accuracy for the same pixels within the six Landsat scenes ranged from 7% to 53% (average 39%). This is a somewhat unfair comparison, since the accuracy assessment was designed for the 1 km-pixels of the Raster CAVM, and not the more generalized polygons of the original CAVM, but it does demonstrate the improvements due to both the greater resolution and improved mapping of the Raster CAVM.

The evaluation of six contemporary Landsat scenes provides some estimate of the overall accuracy of the Raster CAVM, a comparison of the accuracy of different parts of the map, and the relative accuracy of different map units. However, it is important to recognize that there was no actual ground truth in this evaluation of the Raster CAVM. Interpreting the land cover of the 1-km pixels that made up the Raster CAVM from the Landsat imagery was difficult. The 1-km resolution meant that most pixels were “mixed pixels,” including more than one map unit. Further, Landsat 30-m resolution imagery was often not detailed enough to interpret the land cover of low-statured arctic vegetation types. This was especially noticeable in the accuracy assessment of the erect shrub type (S1), which intergrades with several other types (prostrate and hemi-prostrate shrub tundra, P1 and P2; non-tussock- and tussock graminoid-shrub tundra, G3 and G4). Geolocation issues between the Landsat imagery and the Raster CAVM also likely caused additional problems (Strahler et al., 2006).

We considered the alternatives of using actual ground data, or a comparison using existing maps. The available ground data are few, unevenly distributed across the Arctic, and especially lacking in Canada and Russia. The large extent of the map and the difficulties of getting independent, relevant, accurate data (Loew et al., 2017) made ground truthing impossible. Other researchers have had similar difficulty in the Arctic. The Circa 2010 Land Cover of Canada, based on 30-m Landsat data, included an accuracy assessment, but the authors acknowledged that it was not very good for the arctic portion, due to a lack of data (Latifovic et al., 2017). The variation in the availability of maps, and the difficulty of cross-walking disparate regional land cover classifications to the CAVM legend made the map comparison option unworkable. In addition, the best available ground maps were used as ancillary data to verify and improve the Raster CAVM, so they could not be used for an independent validation. Finally, there was no assurance that these existing maps were any more correct than the Raster CAVM.

Areas of the Raster CAVM with few ground data and no local vegetation maps were the most difficult to map, and showed the lowest accuracies (e.g. Kolyma Delta, 58%). This included large areas of the Russian Arctic and parts of the Canadian Arctic. In these remote areas, ground photos that were part of the Google Earth “Panaramio” geolocated photo sharing application were especially helpful for improving the accuracy of the mapping. Numerous guides and arctic travelers posted their photos in this way. Google Earth has since switched to a different photo-sharing platform, which focused on commercial businesses, and removed all Panaramio photos. Responding to user complaints, they have slowly been reposting photos from remote areas (Google Product Forum, 2018).

We emphasize that the purpose of the Raster CAVM project was to produce a map with a realistic pattern and distribution of land cover types at circumpolar, continental, and broad regional scales. It was not designed to be used at the pixel scale for ground plot selection or other applications that required high pixel-by-pixel accuracy. The overall accuracy of 70% shows that the data set, when used as a whole, is quite robust. Most importantly, all of the regional experts involved in the production of the Raster CAVM agreed that it provided a more accurate

representation of the distribution of vegetation in the portion of the Arctic they knew best than the original CAVM.

4.5. Changing arctic vegetation

The accuracy assessment used the most recently available, cloud-free, summer Landsat imagery (one 2016 scene, three 2017, two 2018) (Table S4). This allowed us to check for changes in vegetation since the time when the imagery used for the classification was collected (1993–1995, AVHRR and 2000–2009, MODIS), to see if the map accurately shows current conditions in the Arctic. The most common large-scale changes in arctic vegetation reported in the literature are an increase in shrubs (Myers-Smith et al., 2015) and increases in ice-wedge thermokarst and small water bodies (Liljedahl et al., 2016). The accuracy assessment did not reveal any large-scale shifts towards more shrubby or wetter vegetation units within this time-frame (Tables S6–S11).

This result increases confidence that the map properly portrays the current arctic vegetation, but does not mean that arctic vegetation is not changing. Both the spatial resolution and the legend resolution of the Raster CAVM are too coarse for monitoring changing arctic vegetation. Incremental changes, such as increased shrub height, could occur without changing the mapping unit for an area. Changes are occurring most rapidly within successional environments (e.g., floodplains, Tape et al., 2012) and ice-wedge polygon troughs (Liljedahl et al., 2016), at scales that are smaller than the 1-km resolution of the Raster CAVM. The recently documented changes in arctic landscapes related to thawing permafrost, such as thermokarst ponds (Liljedahl et al., 2016), thaw slumps (Nitze et al., 2018), and subsidence (Farquharson et al., 2019) are occurring over wide areas. These changes cause subtle changes in satellite signatures, best identified with finer resolution imagery and statistical analysis (e.g. Raynolds and Walker, 2016).

5. Conclusion

Most available circumpolar land cover maps of the Arctic based on satellite imagery have very limited legends that do not convey the spatial variability or ecological relevance needed for applications such as climate, carbon flux, surface energy balance, or permafrost modeling (Bartsch et al., 2016). The original CAVM legend had the appropriate level of detail, but its spatial resolution was relatively coarse (14-km polygons) and in a vector format. The new Raster CAVM addresses both those problems, building on the strengths of the original CAVM and improving its spatial resolution and accuracy.

The Raster CAVM has the same legend as the original CAVM (though the barren complex used to map the Canadian Shield was split into two sub-types), the same extent and projection, and has a 1-km spatial resolution. The new map was able to distinguish water-bodies and vegetation within mountain ranges in more detail than the original. The Raster CAVM shows four-times as much water cover as the original CAVM. The new map shows less cover of low shrubs (> 40 cm tall) than the original CAVM, a result of bringing in new information from local maps and regional expertise. The NDVI, elevation, and summer temperature characteristics of the different map units showed inter-related patterns.

The Raster CAVM GIS data are freely available on the web (geobotany.uaf.edu and at Mendeley Data, DOI: 10.17632/c4xj5rv6kv.1). It is an appropriate data resource for representing arctic land cover in circumpolar and regional models of subjects such as climate, permafrost, and species distribution. Future revisions of the Raster CAVM should include improved treeline, coast, and glacial boundaries, as well as improvements in mapping based on new remotely sensed variables and imagery, and any new regional mapping.

Acknowledgements

Our thanks to Jana Müllerová for discussions of accuracy assessments, and two anonymous reviewers and the journal editor for comments and suggestions which improved the paper. Funding for this project was provided mostly by the NASA Land Cover and Land Use Change Program (LCLUC Grant No. NNX14AD90G). Additional support was provided by the NASA Pre-ABoVE Program (Grant No. NNX13AM20G), NASA ABoVE program (Contract No. NNH16CP09C), NSF Arctic Science, Engineering and Education for Sustainability (ARCSEES Grant No. 1263854), NSF Arctic System Science (ARCSS Award No. 1737750), and the Russian Foundation for Basic Research (Grant No. 18-04-01010 A). We appreciate the international support from the Conservation of Arctic Flora and Fauna (CAFF) Working Group of the Arctic Council for both the original Circumpolar Arctic Vegetation Map (CAVM) and for the Raster CAVM.

Appendix A. Supplementary data

Supplementary data to this article can be found online at https://doi.org/10.1016/j.rse.2019.111297.

References

Aaron-Morrison, A.P., Ackerman, S.A., Adams, N.G., Adler, R.F., Albanil, A., Alfaro, E.J., et al., 2016. State of the climate in 2015. Bull. Am. Meteorol. Soc. 97, S1–S275.

AMAP, 2017. Snow, Water, Ice and Permafrost in the Arctic (SWIPA) 2017 (p. xiv + 269 pp). Arctic Monitoring and Assessment Programme (AMAP), Oslo, Norway.

AMAP, 2018. Adaptation Actions for a Changing Arctic: Barents Area. Arctic Monitoring and Assessment Programme (AMAP), Oslo, Norway, pp. 24.

Bartsch, A., Höfler, A., Kroisleitner, C., Trofaier, A.M., 2016. Land cover mapping in northern high latitude permafrost regions with satellite data: achievements and remaining challenges. Remote Sens. 8, 979.

Blok, D., Schaepman-Strub, G., Bartholomeus, H., Heijmans, M.M.P.D., Maximov, T.C., Berendse, F., 2011. The response of Arctic vegetation to the summer climate: relation between shrub cover, NDVI, surface albedo and temperature. Environ. Res. Lett. 6, 035502 (035509pp).

Box, J.E., Colgan, W.T., Christensen, T.R., Schmidt, N.M., Lund, M., Parmentier, F.-J.W., Brown, R.D., Bhatt, U.S., Euskirchen, E.S., Romanovsky, V.E., Walsh, J.E., Overland, J.E., Wang, M., Corell, R.W., Meier, W.N., Wouters, B., Mernild, S., Mård, J., Pawlak, J., Olsen, M.S., 2019. Key indicators of Arctic climate change: 1971–2017. Environ. Res. Lett. 14, 045010.

Braun-Blanquet, J., 1928. Pflanzensoziologie, 7.1 ed. Grundzüge der Vegetationskunde, Berlin.

Brossard, T., Joly, D., 1994. Probability models, remote sensing and field observation: test for mapping some plant distributions in the Kongsfjord area, Svalbard. Polar Res. 13, 153–161.

CAVM Team, 2003. Circumpolar Arctic Vegetation Map, scale 1:7 500 000. In: Conservation of Arctic Flora and Fauna (CAFF) Map No. 1. U.S. Fish and Wildlife Service, Anchorage, Alaska.

Davidson, S.J., Santos, M.J., Sloan, V.L., Watts, J.D., Phoenix, G.K., Oechel, W.C., Zona, D., 2016. Mapping arctic tundra vegetation communities using field spectroscopy and multispectral satellite data in North Alaska, USA. Remote Sens. 8, 978.

Epstein, H.E., Walker, D.A., Raynolds, M.K., Jia, G.J., Kelley, A.M., 2008. Phytomass patterns across a temperature gradient of the north American arctic tundra. J. Geophys. Res. 113, G03S02.

ESRI, 1993. Digital Chart of the World. Environmental Systems Research Institute, Inc, Redlands, CA.

ESRI, 2010. ArcGIS Desktop Help 10.0 – How Iso Cluster Works. Available online at. http://desktop.arcgis.com/en/arcmap/10.3/tools/spatial-analyst-toolbox/how-iso-cluster-works.htm, Accessed date: 2 April 2019.

European Commission, J.R.C, 2003. Global Land Cover 2000 Database (GLC 2000). http://forobs.jrc.ec.europa.eu/products/glc2000/glc2000.php.

Farquharson, L.M., Romanovsky, V.E., Cable, W.L., Walker, D.A., Kokelj, S.V., Nicolsky, D.J., 2019. Climate change drives widespread and rapid thermokarst development in very cold permafrost in the Canadian high Arctic. Geophys. Res. Lett. https://doi.org/10.1029/2019GL082187.

Google Product Forum, 2018. What happened to Google Earth old Panoramio photos that users uploaded? https://support.google.com/maps/forum/AAAAQuUrST8H4VObBFsIyA/?hl=en&gpf=%23!msg%2Fmaps%2FH4VObBFsIyA%2FnZ8Aod3sBAAJ&msgid=nZ8Aod3sBAAJ, Accessed date: 26 June 2018.

Hoegh-Guldberg, O., Jacob, D., Taylor, M., Bindi, M., Brown, S., Camilloni, I., Diedhiou, A., Djalante, R., Ebi, K.L., Engelbrecht, F., Guiot, J., Hijioka, Y., Mehrotra, S., Payne, A., Seneviratne, S.I., Thomas, A., Warren, R., Zhou, G., 2018. Chapter 3: Impacts of 1.5°C global warming on natural and human systems. In: Masson-Delmotte, V., Zhai, P., Pörtner, H.-O., Roberts, D., Skea, J., Shukla, P.R., Pirani, A., Moufouma-Okia, W., Péan, C., Pidcock, R., Connors, S., Matthews, J.B.R., Chen, Y., Zhou, X., Gomis, M.I.,

Lonnoy, E., Maycock, T., Tignor, M., Waterfield, T. (Eds.), Global Warming of 1.5 °C. an IPCC Special Report on the Impacts of Global Warming of 1.5°C above Pre-Industrial Levels and Related Global Greenhouse Gas Emission Pathways, in the Context of Strengthening the Global Response to the Threat of Climate Change, Sustainable Development, and Efforts to Eradicate Poverty. Intergovernmental Panel on Climate Change.

Hoffman, M.H., 2011. Not across the North Pole: plant migration in the Arctic. New Phytol. 2011. https://doi.org/10.1111/j.1469-8137.2011.03924.x.

IPCC, 2014. Climate Change 2014: Synthesis Report. Contribution of Working Groups I. II and III to the Fifth Assessment Report of the Intergovernmental Panel on Climate Change, Geneva, Switzerland.

Jorgenson, M.T., Meidinger, D., 2015. The Alaska-Yukon region of the circumboreal vegetation map (CBVM). In: Conservation of Arctic Flora and Fauna. CAFF, Akureyri, Iceland.

Joria, P.E., Jorgenson, J.C., 1996. Comparison of three methods for mapping tundra with Landsat digital data. Photogramm. Eng. Remote Sens. 62, 163–169.

Kankaanpää, P., Young, O.R., 2012. The effectiveness of the Arctic Council. Polar Res. 31, 17176.

Koroleva, N.E., 1994. Phytosociological survey of the tundra vegetation of the Kola Peninsula, Russia. J. Veg. Sci. 5, 803–812.

Krankina, O.N., Pflugmacher, D., Hayes, D.J., McGuire, A.D., Hansen, M.C., Häme, T., Elsakov, V., Nelson, P., 2011. Vegetation cover in the Eurasian Arctic: distribution, monitoring, and role in carbon cycling. In: Gutman, G., Reissell, A. (Eds.), Eurasian Arctic Land Cover and Land Use in a Changing Climate. Springer, New York, pp. 79–108.

Langford, Z., Kumar, J., Hoffman, F.M., Norby, R.J., Wullschleger, S.D., Sloan, V.L., Iversen, C.M., 2016. Mapping arctic plant functional fype distributions in the Barrow Environmental Observatory using WorldView-2 and LiDAR datasets. Remote Sens. 8, 733.

Latifovic, R., Pouliot, D., Olthof, I., 2017. Circa 2010 land cover of Canada: local optimization methodology and product development. Remote Sens. 9, 1098.

Liljedahl, A.K., Boike, J., Daanen, R.P., Fedorov, A.N., Frost, G.V., Grosse, G., Hinzman, L.D., Iijma, Y., Jorgenson, J.C., Matveyeva, N.V., Nescoiu, M., Raynolds, M.K., Romanovsky, V.E., Schulla, J., Tape, K.D., Walker, D.A., Wilson, C.J., Yabuki, H., Zona, D., 2016. Pan-Arctic ice-wedge degradation in warming permafrost and its influence on tundra hydrology. Nat. Geosci. https://doi.org/10.1038/NGEO2674.

Loew, A., Bell, W., Brocca, L., Bulgin, C.E., Burdanowitz, J., Calbet, X., Donner, R.V., Ghent, D., Gruber, A., Kaminski, T., Kinzel, J., Klepp, C., Lambert, J.C., Schaepman-Strub, G., Schröder, M., Verhoels, T., 2017. Validation practices for satellite-based Earth observation data across communities. Rev. Geophys. 55, 779–817.

Loranty, M.M., Goetz, S.J., Beck, P.S.A., 2011. Tundra vegetation effects on pan-Arctic albedo. Environ. Res. Lett. 6, 024014 (024017pp).

Macander, M.J., Swingley, C.S., Joly, K., Raynolds, M.K., 2015. Landsat-based snow persistence map for northwest Alaska. Remote Sens. Environ. 163, 23–31.

Macander, M.J., Frost, G.V., Nelson, P.R., Swingley, C.S., 2017. Regional quantitative cover mapping of tundra plant functional types in Arctic Alaska. Remote Sens. 9, 1024.

Maes, J., Egoh, B., Willemen, L., Liquete, C., Vihervaara, P., Schägner, J.P., Grizzetti, B., Drakou, E.G., La Notte, A., Zulian, G., Bouraoui, F., 2012. Mapping ecosystem services for policy support and decision making in the European Union. Ecosystem Services 1, 31–39.

Marceau, D.J., 1999. The scale issue in the social and natural sciences. Can. J. Remote. Sens. 25, 347–356.

Markon, C.J., Fleming, M.D., Binnian, E.F., 1995. Characteristics of vegetation phenology over the Alaskan landscape using AVHRR time-series data. Polar Record 31, 179–190.

Montesano, P.M., Neigh, C.S.R., Sexton, J.O., Feng, M., Channan, S., Ranson, K.J., Townshend, J.R.G., 2016. Calibration and validation of Landsat tree cover in the taiga-tundra ecotone. Remote Sens. 8, 551.

Montesano, P.M., Neigh, C.S.R., Sun, G., Duncanson, L., Van Den Hoek, J., Ranson, K.J., 2017. The use of sun elevation angle for stereogrammetric boreal forest height in open canopies. Remote Sens. Environ. 196, 76–88.

Moulton, M.A., Hesp, P.A., Miot da Silva, G., Bouchez, C., Lavy, M., Fernandez, G.B., 2019. Changes in vegetation cover on the Younghusband Peninsula transgressive dunefields (Australia) 1949–2017. Earth Surf. Process. Landf. 44, 459–470.

Myers-Smith, I.H., Beck, P.S.A., Wilmking, M., Hallinger, M., Blok, D., Tape, K., Rayback, S.A., Macias-Fauria, M., Forbes, B.C., Speed, J.D.M., Boulanger-Lapointe, N., Rixen, C., Lévesque, E., Schmidt, N.M., Baittinger, C., Trant, A.J., Hermanutz, L., Collier, L.S., Dawes, M.A., Lantz, T.C., Weijers, S., Jørgensen, R.H., Buchwal, A., Buras, A., Naito, A.T., Ravolainen, V., Schaepman-Strub, G., Wheeler, J.A., Wipf, S., Guay, K.C., Hik, D.S., Vellend, M., 2015. Climate sensitivity of shrub growth across the tundra biome. Nat. Clim. Chang. 5, 887–891.

Nitze, I., Grosse, G., Jones, B.M., Romanovsky, V.E., Boike, J., 2018. Remote sensing quantifies widespread abundance of permafrost region disturbances across the Arctic and Subarctic. Nat. Commun. 9, 5423.

Olthof, I., Fraser, R.H., 2007. Mapping northern land cover fractions using Landsat ETM +. Remote Sens. Environ. 107, 496–509.

Overpeck, J., Hughen, K., Hardy, D., Bradley, R., Case, R., Douglas, M., Finney, B., Gajewski, K., Jacoby, G., Jennings, A., Lamoureux, S., Lasca, A., MacDonald, G., Moore, J., Retelle, M., Smith, S., Wolfe, A., Zielinski, G., 1997. Arctic environmental change of the last four centuries. Science 278, 1251–1256.

Pearson, R.G., Phillips, S.J., Loranty, M.M., Beck, P.S.A., Damoula, T., Knight, S.J., Goetz, S.J., 2013. Shifts in Arctic vegetation and associated feedbacks under climate change. Nat. Clim. Chang. https://doi.org/10.1038/NCLIMATE1858.

Pfalz, G., 2017. Lateral Transport of Sediment and Organic Matter, Derived from Coastal Erosion, into the Nearshore Zone of the Southern Beaufort Sea, Canada. Alfred Wegener Institute for Polar and Marine Research.

Ping, C.-L., Michaelson, G.J., Jorgenson, M.T., Kimble, J.M., Epstein, H.E., Romanovsky, V.E., Walker, D.A., 2008. High stocks of soil organic carbon in the North American Arctic region. Nat. Geosci. 1, 615–619.

Raynolds, M.K., Walker, D.A., 2016. Increased wetness confounds Landsat-derived NDVI trends in the central Alaska North Slope region, 1985-2011. Environ. Res. Lett. 11, 085004.

Raynolds, M.K., Walker, D.A., Maier, H.A., 2006. NDVI patterns and phytomass distribution in the circumpolar Arctic. Remote Sens. Environ. 102, 271–281.

Raynolds, M.K., Comiso, J.C., Walker, D.A., Verbyla, D., 2008a. Relationship between satellite-derived land surface temperatures, arctic vegetation types, and NDVI. Remote Sens. Environ. 112, 1884–1894.

Raynolds, M.K., Walker, D.A., Munger, C.A., Vonlanthen, C.M., Kade, A.N., 2008b. A map analysis of patterned-ground along a North American Arctic transect. J. Geophys. Res. 113, G03S03. https://doi.org/10.1029/2007JG000512.

Schuur, E.A.G., Abbott, B.W., Bowden, W.B., Brovkin, V., Camill, P., Canadell, J., Chanton, J.P., Chapin III, F.S., Christensen, T.R., Ciais, P., Crosby, B.T., Czimczik, C.I., Grosse, G., Harden, J., Hayes, D.J., Hugelius, G., Jastrow, J.D., Jones, J.B., Kleinen, T., Koven, C.D., Krinner, G., Kuhry, P., Lawrence, D.M., McGuire, A.D., Natali, S.M., O'Donnell, J., Ping, C.L., Riley, W.J., Rinke, A., Romanovsky, V.E., Sannel, A.B.K., Shadel, C., Schaefer, K., Sky, J., Subin, Z.M., Tarnocai, C., Turetsky, M.R., Waldrop, M., Anthony Walter, K.M., Wickland, K.P., Wilson, C.J., Zimov, S.A., 2013. Expert assessment of vulnerability of permafrost carbon to climate change. Clim. Chang. https://doi.org/10.1007/s10584-013-0730-7.

Strahler, A.H., Boschetti, L., Foody, G.M., Friedl, M.A., Hansen, M.C., Herold, M., Mayaux, P., Morisette, J.T., Stehman, S.V., Woodcock, C.E., 2006. Global Land Cover Validation: Recommendations for Evaluation and Accuracy Assessment of Global Land Cover Maps. European Communities, Luxembourg.

Sturm, M., Douglas, T., Racine, C.H., Liston, G.E., 2005. Changing snow and shrub conditions affect albedo with global implications. J. Geophys. Res. 110. https://doi.org/10.1029/2005JG000013.

Takeuchi, W., Tamura, M., Yasuoka, Y., 2003. Estimation of methane emission from West Siberian wetland by scaling technique between NOAA AVHRR and SPOT HRV. Remote Sens. Environ. 85, 21–29.

Tape, K.D., Hallinger, M., Welker, J.M., Ruess, R.W., 2012. Landscape heterogeneity of shrub expansion in Arctic Alaska. Ecosystems 15, 711–724.

Treat, C.C., Marushchak, M.E., Voigt, C., Zhang, Y., Tan, Z., Zhuang, Q., Virtanen, T.A., Räsänen, A., Biasi, C., Hugelius, G., Kaverin, D., Miller, P.A., Stendel, M., Romanovsky, V.E., Rivkin, F., Martikainen, P.J., Shurpali, N.J., 2018. Tundra landscape heterogeneity, not interannual variability, controls the decadal regional carbon balance in the Western Russian Arctic. Glob. Chang. Biol. 1–17. https://doi.org/10.1111/gcb.14421.

Trishchenko, A.P., Luo, Y., Khlopenkov, K.V., Park, W.M., Wang, S., 2009. Arctic circumpolar mosaic at 250m spatial resolution for IPY by fusion of MODIS/TERRA land bands B1–B7. Int. J. Remote Sens. 30, 1635–1641.

Virtanen, T., Ek, M., 2014. The fragmented nature of tundra landscapes. Int. J. Appl. Earth Obs. Geoinf. 27, 4–12.

Walker, D.A., Bay, C., Daniels, F.J.A., Einarsson, E., Elvebakk, A., Johansen, B.E., Kapitsa, A., Kholod, S.S., Murray, D.F., Talbot, S.S., Yurtsev, B.A., Zoltai, S.C., 1995. Toward a new arctic vegetation map: a review of existing maps. J. Veg. Sci. 6, 427–436.

Walker, D.A., Gould, W.A., Raynolds, M.K., 2002. The circumpolar Arctic vegetation map: environmental controls, AVHRR-derived base maps, and integrated mapping procedures. Int. J. Remote Sens. 23, 2551–2570.

Walker, D.A., Raynolds, M.K., Daniels, F.J.A., Einarsson, E., Elvebakk, A., Gould, W.A., Katenin, A.E., Kholod, S.S., Markon, C.J., Melnikov, E.S., Moskalenko, N.G., Talbot, S.S., Yurtsev, B.A., CAVM Team, 2005. The circumpolar Arctic vegetation map. J. Veg. Sci. 16, 267–282.

Walker, D.A., Daniels, F.J.A., Alsos, I.G., Bhatt, U.S., Breen, A.L., Buchhorn, M., Bueltmann, H., Druckenmiller, L.A., Edwards, M.E., Ehrich, D., 2016. Circumpolar Arctic vegetation: a hierarchic review and roadmap toward an internationally consistent approach to survey, archive and classify tundra plot data. Environ. Res. Lett. 11, 055005.

Walker, D.A., Daniëls, F.J.A., Matveyeva, N.V., Šibík, J., Walker, M.D., Breen, A.L., Druckenmiller, L.A., Raynolds, M.K., Bültmann, H., Hennekens, S., Buchhorn, M., Epstein, H.E., Ermokhina, K.A., Fosaa, A.M., Heiðmarsson, S., Heim, B., Jónsdóttir, I.S., Koroleva, N., Levesque, E., MacKenzie, W.H., Henry, G.H.R., Nilsen, L., Peet, R.K., Razzhivin, V.Y., Talbot, S.S., Telyatnikov, M., Thannheiser, D., Webber, P.J., Wirth, L.W., 2018. Circumpolar arctic vegetation classification. Phytocoenologia 48, 181–201.

Yurtsev, B.A., 1994. Floristic divisions of the Arctic. J. Veg. Sci. 5, 765–776.

Zhang, C.-s., Li, H., 2012. The estimation of sub-pixel NDVI time series based on downscaling technique. In: Cao, Z., Fenster, A., Nyul, L., Cai, C. (Eds.), MIPPR 2011: Multispectral Image Acquisition, Processing and Analysis.

Zhang, W., Witharana, C., Liljedahl, A.K., Kanevskiy, M., 2018. Deep convolutional neural networks for automated characterization of arctic ice-wedge polygons in very high spatial resolution aerial imagery. Remote Sens. 10, 1487.